Joint Estimation Algorithms for Cochannel Signal Demodulation

K. Giridhar† Sujai Chari‡ John J. Shynk† Richard P. Gooch‡ Douglas J. Artman‡

† Center for Information Processing Research
Dept. of Elec. and Comp. Engineering
University of California
Santa Barbara, CA 93106

‡ Applied Signal Technology, Inc.
160 Sobrante Way
Sunnyvale, CA 94086

Abstract

Nonlinear algorithms for the joint recovery of cochannel narrowband signals are proposed. For finite impulse response channel characteristics, maximum likelihood and maximum a posteriori criteria are employed to derive cochannel demodulators of varying complexities and degrees of performance. The error rate performance of these joint estimation algorithms is examined through computer simulations.

1 Introduction

Cochannel interference is a major impairment to reliable transmission in many narrowband communication systems. For example, in cellular radio systems employing frequency-reuse, one or more secondary signals from nearby cells can interfere with the desired (primary) signal. In addition to cochannel interference, the primary and secondary signals may be corrupted by intersymbol interference (ISI) from multipath delays and by additive noise. Among these factors, cochannel interference often causes the most severe degradation in performance due to spectral overlap. Instead of using interference suppression techniques, in certain applications like dual-polarized microwave radio, we are interested in *jointly* estimating both cochannel signals. Spatial diversity techniques for estimating narrowband cochannel signals have been proposed in the array processing literature (e.g., see [1]). In this paper, we are interested in cochannel demodulation using a single receiver, and hence *nonlinear* processing techniques are needed to achieve an acceptable bit error rate (BER) performance.

We consider a communication system model with one secondary data stream to be jointly recovered along with the primary data stream. The techniques are based on maximum likelihood sequence estimation (MLSE) [2] and maximum a posteriori symbol detection (MAPSD) [3]. Since the cochannel data sequences are jointly recovered, we refer to the corresponding algorithms as joint MLSE (JMLSE) and joint MAPSD (JMAPSD). These optimal techniques can be expected to yield the best possible BER performance under a wide range of signal and channel conditions, but they are computationally expensive. However, it is possible to implement the JMAPSD algorithm using a suboptimal two-stage configuration (which has some similarity to a quasi-linear "demod-remod" approach proposed in [4]), thereby reducing the computational complexity. Also, a novel secondary feedback mechanism can be incorporated into the two-stage JMAPSD algorithm, which greatly enhances its BER performance for low signal-to-interference ratios (SIRs).

*This work was sponsored in part by Applied Signal Technology, Inc., and the University of California MICRO Program.

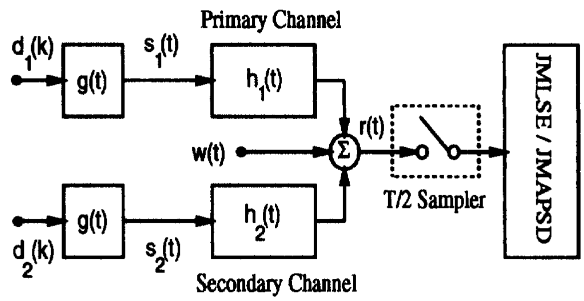

Figure 1: Cochannel system model.

2 Cochannel Signal Model

The assumed cochannel system model is shown in Figure 1. The transmitted low-pass equivalent waveforms can be represented by

$$s_m(t) = \sum_{k=-\infty}^{\infty} d_m(k)g(t-kT), \; m = 1,2 \qquad (1)$$

where T is the symbol duration, and $\{d_1(k)\}$ and $\{d_2(k)\}$ are the primary and secondary source symbols, respec-

0-7803-0950-2/93/$3.00©1993IEEE

tively. The pulse function $g(t)$ has a raised-cosine response with a finite duration of $2T$ seconds. We propose a $T/2$-spaced sampler implementation (although it has about twice the complexity of a T-spaced implementation) for the following reasons: (a) eliminates the need for a whitening matched filter (which cannot be ideally defined for this cochannel problem); (b) takes advantage of the excess bandwidth in $g(t)$; and (c) reduces sensitivity to sampling time offsets, and thus recovers nonsynchronized cochannel signals more easily than a T-spaced implementation.

Hence, the discrete measurement samples of the received signal $r(t)$ at the output of the $T/2$-spaced sampler in Figure 1 are given by

$$r(kT + jT/2) = \sum_{m=1}^{2} \sum_{n=0}^{L_m} f_{m,n}(kT + jT/2) d_m(k-n) + w(kT + jT/2), \;\; j = 0, 1 \qquad (2)$$

where the noise sequences $\{w(kT + jT/2)\}$ are assumed to be mutually uncorrelated, white, and Gaussian with zero mean and equal variance σ_w^2. The delay spreads of the primary and secondary channels are L_1T and L_2T, respectively. The $2(L_m + 1)$ channel coefficients $\{f_{m,n}(kT + jT/2)\}$ represent the convolution of the ISI channels $\{h_m(t)\}$ with the transmit filter $g(t)$, sampled at $T/2$ seconds (assuming perfect timing synchronization). For convenience, we will henceforth use a T-spaced representation for all variables; for example, we will use $r(k)$ instead of $r(kT + jT/2)$. The goal of the receiver is to accurately recover the primary and secondary sequences $\{d_1(k)\}$ and $\{d_2(k)\}$, given reliable estimates of the channel coefficients $\{f_{1,n}(k)\}$ and $\{f_{2,n}(k)\}$.

3 Joint ML Sequence Estimation

In the single-channel scenario, the objective of MLSE it to determine the one sequence $d_i^k = \{d_i(k), \ldots, d_i(0)\}$ out of all possible transmitted symbol sequences such that

$$p(r^k | d_i^k) \geq p(r^k | d_q^k), \forall q \neq i \qquad (3)$$

where $r^k = \{r(k), \ldots, r(0)\}$ is the actual received sequence. When the additive noise components in (2) are independent and Gaussian, the above can be replaced by a Euclidean distance criterion, which for T-spaced MLSE is given by

$$d_i^k : \sum_{l=0}^{k} |r(l) - \hat{r}_i(l)|^2 \geq \sum_{l=0}^{k} |r(l) - \hat{r}_q(l)|^2, \forall q \neq i \qquad (4)$$

where $\hat{r}_i(k)$ are the signal estimates generated from d_i^k using the known channel coefficients. (In $T/2$-spaced MLSE, the single summations become double summations, analogous to that in (2).) For the joint demodulation of two

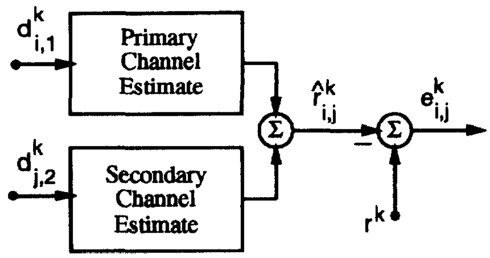

Figure 2: Joint ML sequence estimation.

cochannel signals, the objective of JMLSE (illustrated in Figure 2) is to determine the *pair* of sequences $\{d_{i,1}^k, d_{j,2}^k\}$ that minimize the sum of squared errors defined by the error (likelihood) sequence $e_{i,j}^k$.

When the channel has a finite impulse response (FIR), the Viterbi algorithm (VA) is a practical way of implementing optimal (single-channel) MLSE [2]. Assuming a channel memory of L symbol lengths, the VA maintains a decoding trellis with M^L nodes or states (where M is the number of source symbols) and an equal number of survivor sequences. Each state is a particular sequence of L previously transmitted symbols $\{d(k-1), \ldots, d(k-L)\}$ from which the present symbol $d(k)$ could be obtained. For example, the i^{th} state is defined by $s_i^{k-1,L} = \{d_i(k-1), \ldots, d_i(k-L)\}$; it is evident that $s_i^{k-1,L}$ can transition to M possible states at time k, and that it could have been reached from M different states at time $k-2$. The VA decisions are computed by truncating the survivors after $4L - 5L$ symbols [2].

The Viterbi algorithm for JMLSE is implemented in a method very similar to that of the single-channel VA. A joint state $S_i^{k-1,L} = [s_{i,1}^{k-1,L_1} \; s_{i,2}^{k-1,L_2}]$ is defined by appending the primary ($s_{i,1}^{k-1,L_1}$) and secondary ($s_{i,2}^{k-1,L_2}$) states. Observe that in this case, each joint state at time $k-1$ can transition to M^2 states at time k and can be reached by the same number of states from time $k-2$. Hence, the number of states required to implement the optimal joint VA is $M^{L_1+L_2}$. For high-order signal constellations (e.g., 16-PSK or 64-QAM), complexity reduction techniques originally developed for single-channel MLSE, such as reduced-state sequence estimation (RSSE) [5], may be employed for JMLSE. A discussion of this approach is beyond the scope of this paper, but we expect that RSSE will be beneficial for the case of minimum-phase type channels.

4 Joint MAP Symbol Detection

The MAP symbol-by-symbol decoding scheme [3] minimizes the probability of a symbol error, i.e.,

$$J = \max_{d(k-L)} p(d(k-L)|r^k), \quad (5)$$

and theoretically can provide more reliable decisions than the VA for the *same* decoding delay. The MAPSD algorithm maintains a MAP metric $p(d_i^{k,L}|r^k)$ for every subsequence of length $L+1$ defined by $d_i^{k,L} = \{d_i(k), \ldots, d_i(k-L)\}$. By utilizing the FIR nature of the channel, (5) can be expressed as

$$J = \max_{d(k-L)} \sum_{d(k)} \cdots \sum_{d(k-L+1)} p(d^{k,L}|r^k), \quad (6)$$

and the recursion to calculate the i^{th} MAP metric $p(d_i^{k,L}|r^k)$ is

$$p(d_i^{k,L}|r^k) = \frac{1}{c} p(r(k)|d_i^{k,L}) \; q_i(k-1). \quad (7)$$

The predecessor metric is given by

$$q_i(k-1) = \sum_{\{j: d_j^{k-1,L} \in d_i^{k,L}\}} p(d_j^{k-1,L}|r^{k-1}), \quad (8)$$

$c = Mp(r(k)|r^{k-1})$ is a normalization constant, and $p(r(k)|d_i^{k,L})$ is a Gaussian pdf (likelihood). The summation defining $q_i(k-1)$ is performed over the MAP metrics of all possible subsequences at time $k-1$ from which $d_i^{k,L}$ could have been obtained. The corresponding detection algorithm was first derived in [3] for *known* channels, and was recently extended to blind equalization for unknown channels [6].

The complexity of the single-channel MAPSD algorithm is roughly the same order as that of the Viterbi algorithm for MLSE. (Note that although the VA maintains M^L states, it calculates the same number of likelihoods as MAPSD with M^{L+1} subsequences.) A suboptimal MAP rule was introduced in [6] to make a decision on the $(k-L)^{th}$ symbol (at time k) according to $\hat{d}(k-L) = \hat{d}_i(k-L)$ where

$$\hat{d}_i^{k,L} = \arg\max_{d_i^{k,L}} p(d_i^{k,L}|r^k). \quad (9)$$

It is possible to reduce the complexity of the MAPSD algorithm by introducing decision feedback. This MAP/decision-feedback (MAP/DF) algorithm [7] provides a performance-complexity tradeoff, ranging from that of the full MAP estimator to the conventional decision-feedback equalizer (DFE).

For cochannel symbol detection, an optimal JMAPSD algorithm (of complexity $M^{L_1+L_2+2}$) can be obtained by modifying the single-channel MAPSD algorithm above, and it provides a BER performance comparable to that of JMLSE. However, a computational advantage is obtained when this single-stage JMAPSD structure is reconfigured as a *two-stage* algorithm, as illustrated in Figure 3. The first MAP section models the M^{L_1+1} subsequences of the primary channel; the subsequence decisions $\hat{d}_{1,max}^{k,L_1}$ are obtained from (9) to compute the primary signal estimate

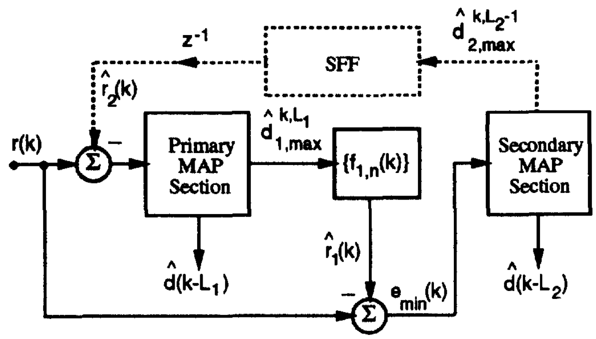

Figure 3: Two-stage JMAPSD algorithm.

$$\hat{r}_1(k) = \sum_{n=0}^{L_1} f_{1,n}(k)\hat{d}_{1,max}(k-n). \quad (10)$$

The residual error $e_{min}(k) = r(k) - \hat{r}_1(k)$ becomes the input of the second MAP section, which models the M^{L_2+1} subsequences of the secondary channel. Hence, the complexity of two-stage JMAPSD is only on the order of $M^{L_1+1} + M^{L_2+1}$. The assumption here is that the SIR is sufficiently large such that the primary MAP metrics converge; thus, cancellation of the primary signal component is nearly complete, and $e_{min}(k)$ contains only the secondary signal component (plus additive noise).

However, by using a feedback filter to subtract a partial estimate of the secondary signal, the two-stage JMAPSD algorithm can also be operated in low-to-medium SIR conditions. The operation of this secondary feedback filter (SFF), also shown in Figure 3, is described below.

1. At time $k-1$, the second MAP stage computes suboptimal decisions on the L_2+1 symbols $\hat{d}_{2,max}^{k-1,L_2}$ using (9).

2. The *first* L_2 secondary symbol decisions are fed en-bloc into the SFF (whose coefficients equal the *last* L_2 values of the secondary channel) to compute

$$\hat{r}_2(k) = \sum_{n=1}^{L_2} f_{2,n}(k-1)\hat{d}_{2,max}(k-n). \quad (11)$$

Hence, $\hat{r}_2(k)$ is an estimate of the secondary interference from all previous symbols excluding the current transmitted symbol $d_2(k)$.

3. At time k, the difference signal $r(k) - \hat{r}_2(k)$ is processed by the primary MAP section.

4. The secondary MAP section input $e_{min}(k)$ is determined as described earlier.

Although the SFF may introduce some error propagation due to decision feedback, for low SIR simulations we obtain a significant improvement in performance. It should also be mentioned that this two-stage JMAPSD structure is different from the one proposed recently by the authors in [8], but is exactly equivalent in function.

5 Computer Simulation Results

The primary and secondary BERs were simulated for these nonlinear algorithms, assuming binary signaling (BPSK). The frequency responses (at baseband) of both channels are shown in Figure 4, where each channel had 14 $T/2$-spaced impulse response samples (provided in [8]). We define $\mathrm{SNR} = 10\log(E_1/N_o)$ and $\mathrm{SIR} = 10\log(E_1/E_2)$ where $E_j = E\{d_j^2(k)\}$ are the signal powers and $N_o/2$ is the noise spectral density. For the algorithms in this study, the signal energies were assumed to be known at the receiver; in particular, we fixed $E_1 = 1$.

The performance of the optimal $M^{2L} = 2^{12} =$ 4096-state JMLSE was compared with the suboptimal *two-stage* JMAPSD$(P_{map}, P_{df}, S_{map}, S_{df})$ algorithm where P_{map} and P_{df} refer to the number of primary (P) channel coefficients modeled by the MAP and DF sections, respectively (similar definitions apply for the secondary (S) channel). For example, JMAPSD(5,1,4,3) is a $2^5 = 32$-state MAP section cascaded with a one-symbol DF filter for the primary channel, and a $2^4 = 16$-state MAP section cascaded with a three-symbol DF filter for the secondary channel.

As a benchmark, the zero-forcing DFE (without a feedforward section) was simulated for cochannel demodulation (which we refer to as a joint DFE (JDFE)), and its BER was determined with detected bits fed back. The secondary feedback mechanism was also incorporated into the JDFE, and the resulting structure resembles that of two-stage JMAPSD in Figure 3 with each MAP/DF section replaced by a single feedback filter. However, in this case the partial estimate of the secondary ISI is obtained directly from the second DF section, and no separate feedback filter is required as in JMAPSD. (We have noticed that for the chosen cochannel coefficients, this JDFE fails to provide acceptable BERs if the secondary feedback mechanism is removed.)

The effect of the SFF at various SIRs on the two-stage JMAPSD(6,1,6,1) algorithm is illustrated in Figure 5 where SNR = 30 dB. Notice that for SIR < 6 dB, the SFF provides more than an order of magnitude improvement in the error rate performance. From the BER curves in Figures 6 and 7, observe that for SIR = 0 dB,

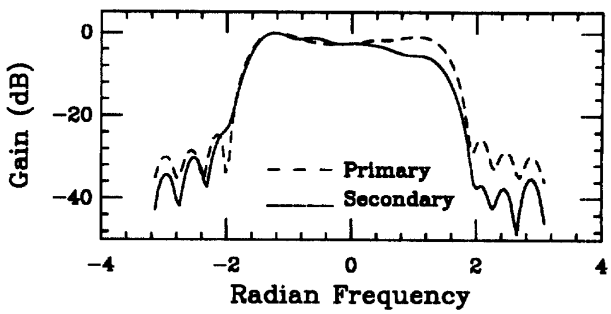

Figure 4: Magnitude response of the channels.

JMLSE provides the best error rate performance, while for SIR = 10 dB, the two-stage JMAPSD algorithm (which includes a SFF) provides nearly the same performance as that of JMLSE (or, equivalently, single-stage JMAPSD). The MAP/DF approach allows for even more computational savings in the JMAPSD algorithm, but at the cost of some performance degradation. Also note that JMAPSD(6,1,6,1) provides SNR gains of about 35 dB at the lower SIR and about 10 dB at the higher SIR compared to the JDFE.

6 Conclusion

Nonlinear joint estimation techniques for the demodulation of narrowband cochannel signals have been presented. For known channels, the Viterbi algorithm for JMLSE and the single-stage JMAPSD algorithm are optimal demodulation techniques that provide the lowest possible BERs. However, for high SIR conditions, the two-stage JMAPSD algorithm has a performance approaching that of JMLSE, but at a much lower complexity. The BER performance of these algorithms exhibits a "near-far" trend similar to that of multiuser detectors in CDMA spread-spectrum systems [9]; i.e., the best *joint* error rates are obtained when the primary and secondary signal energies are comparable. While this work assumes perfect knowledge of the channel impulse responses, extension to unknown channels (blind demodulation) is possible; the corresponding cochannel blind equalization algorithms are proposed in [10].

References

[1] G. Xu, Y. Cho, A. Paulraj, and T. Kailath, "Maximum likelihood detection of co-channel communication signals via exploitation of spatial diversity," in *Proc. Twenty-Sixth Asilomar Conf. on Signals, Systems, and Computers*, (Pacific Grove, CA), pp. 1142–1146, Oct. 1992.

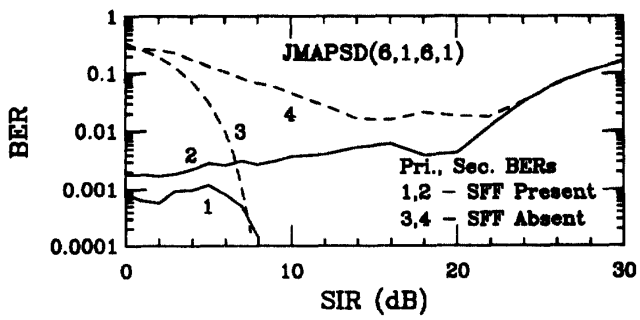

Figure 5: Effect of SFF (SNR = 30 dB).

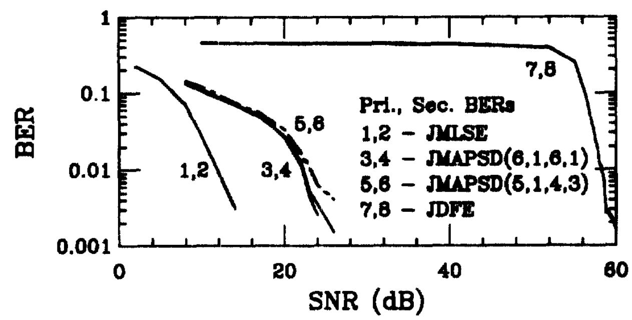

Figure 6: Low SIR condition (SIR = 0 dB).

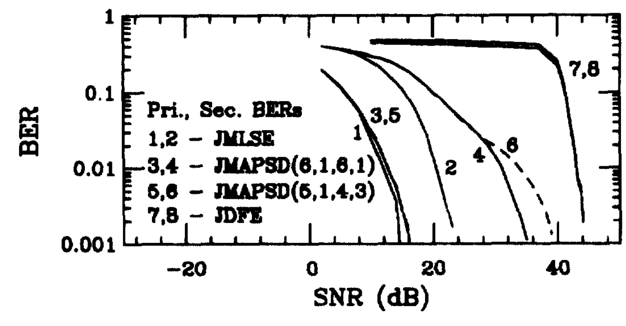

Figure 7: High SIR condition (SIR = 10 dB).

[2] J. G. Proakis, *Digital Communications*. McGraw-Hill, New York, 2nd Ed., 1989.

[3] K. Abend and B. D. Fritchman, "Statistical detection for communication channels with intersymbol interference," *Proc. IEEE*, vol. 58, pp. 779–785, May 1970.

[4] R. P. Gooch and B. J. Sublett, "Demodulation of cochannel QAM signals," in *Proc. IEEE Int. Conf. on Acoustics, Speech, and Signal Processing*, (Glasgow, Scotland), pp. 1392–1395, May 1989.

[5] M. V. Eyuboğlu and S. U. H. Qureshi, "Reduced-state sequence estimation with set partitioning and decision feedback," *IEEE Trans. on Communications*, vol. 36, pp. 13–20, Jan. 1988.

[6] R. A. Iltis, J. J. Shynk, and K. Giridhar, "Recursive Bayesian algorithms for blind equalization," in *Proc. Twenty-Fifth Asilomar Conf. on Signals, Systems, and Computers*, (Pacific Grove, CA), pp. 710–715, Nov. 1991.

[7] K. Giridhar, J. J. Shynk, and R. A. Iltis, "Bayesian/decision-feedback algorithm for blind adaptive equalization," *Optical Engineering*, vol. 31, pp. 1211–1223, June 1992.

[8] K. Giridhar, S. Chari, J. J. Shynk, and R. P. Gooch, "Joint demodulation of cochannel signals using MLSE and MAPSD algorithms," in *Proc. IEEE Int. Conf. on Acoustics, Speech, and Signal Processing*, (Minneapolis, MN), Apr. 1993 (to appear).

[9] S. Verdú, "Recent progress in multiuser detection," in *Advances in Communications and Signal Processing* (A. Porter and S. C. Kak, Eds.), pp. 27–38, Springer-Verlag, New York, 1989.

[10] K. Giridhar and J. J. Shynk, "MAP and ML sequence estimation algorithms for the joint recovery of cochannel signals," *IEEE Trans. on Communications*, 1993 (submitted).